

Graphene in periodic deformation fields: dielectric screening and plasmons

V. K. Dugaev

*Institut für Physik, Martin-Luther-Universität Halle-Wittenberg,
Heinrich-Damerow-Str. 4, 06120 Halle, Germany, and
Department of Physics, Rzeszów University of Technology,
Al. Powstańców Warszawy 6, 35-959 Rzeszów, Poland, and
Department of Physics and CFIF, Instituto Superior Técnico,
Universidade Técnica de Lisboa, Av. Rovisco Pais, 1049-001 Lisbon, Portugal*

M. I. Katsnelson

*Radboud University Nijmegen, Institute for Molecules and Materials,
Heyendaalseweg 135, 6525 AJ Nijmegen, The Netherlands*

(Dated: July 2, 2018)

We consider the effect of periodic scalar and vector potentials generated by periodic deformations of the graphene crystal lattice, on the energy spectrum of electrons. The dependence of electron velocity near the Dirac point on the periodic perturbations of different types is discussed. We also investigated the effect of screening of the scalar potential by calculating the dielectric function as a function of the wave length of the periodic potential. This calculation shows that the periodic scalar field is strongly suppressed by the screening. Using the dependence of electron velocity on the periodic field we also studied the variation of the plasmon spectra in graphene. We found that the spectrum of plasmon excitations can be effectively controlled by the periodic strain field.

PACS numbers: 73.22.pr, 73.21.-b, 71.45.Gm

I. INTRODUCTION

The enormous interest to graphene is related to the unique physical properties of this two-dimensional material¹⁻³, which most possibly will be used in the future in numerous technological applications⁴⁻⁷. An example of such properties of interest for the applications is the existence of very unusual spectrum of plasmon excitations with THz frequencies^{8,9}, that can be used in optoelectronics and communications.

One of the most important problems to be solved to use graphene in electronics is the realization of effective control of the parameters of energy spectrum such as the electron energy gap and/or the velocity of electron and holes. It is already known that by using the electrostatic gating one can vary the carrier density of graphene (i.e., the location of chemical potential). Recently, it was also proposed to use the external strain field to change the energy spectrum – this is called the strain engineering of graphene^{3,10-12}. The idea is mostly based on unusually strong effect of the external deformation acting on the energy spectrum of graphene quite similar to the external electric and magnetic fields^{3,13}.

In this work we consider the effect of periodic fields, which can be generated by periodic deformations, on the energy spectrum, screening of electron-electron interaction, and on the plasmon excitations in graphene. It was already pointed out that such periodic fields do not open the gap near the Dirac point but affect the velocity parameter of electrons and holes¹⁴⁻¹⁶ making the energy spectrum anisotropic. Recently, the effect of periodic modulation on electron spectrum of graphene has been studied experimentally¹⁷. Here we reconsider this

problem in more details, concentrating on possible coexistence of periodic scalar and vector potentials, which, to our knowledge, has not been done before. This is important since a generic deformation produces both scalar and vector potentials^{3,12,13}. We use a different method to solve the problem¹⁸, and find that our numerical results are in agreement with those of Refs. [14,16]. We also discuss the role of screening due to the free carriers in graphene, and we find that screening can substantially suppress the effect of periodic scalar potential.

The combined effect of periodic scalar potential and constant magnetic field in graphene has been recently investigated by Wu et al.¹⁹ They found that the structure of Landau levels can be also strongly affected by the one-dimensional (1D) periodic fields.

The physics of plasmons in graphene has been intensively discussed recently by many authors.²⁰⁻²⁴ The calculations have been performed in frame of standard RPA approximation taking into account the electron energy structure of graphene near the Dirac points, as well as for the whole energy spectrum at the honeycomb lattice²⁵. The effects of magnetic field, finite temperature, chemical potential have been investigated in the same approach²⁶. In this work we discuss the effect of external periodic fields on the screening and on the energy spectrum of plasmons.

II. ELECTRON ENERGY SPECTRUM IN PERIODIC FIELDS

We consider first the transformation of electron energy spectrum related to deformations of the graphene lattice. It is known that the deformation of graphene

is equivalent to the generation of electric and magnetic fields, which can be described by scalar $V(\mathbf{r})$ and vector $\mathbf{A}(\mathbf{r})$ potentials^{3,13}. The relations between the components of strain tensor $u_{ij}(\mathbf{r})$ and the scalar and vector gauge potentials are^{27,28}

$$\begin{aligned} V(\mathbf{r}) &= g(u_{xx} + u_{yy}), \\ A_x(\mathbf{r}) &= \frac{\beta t}{a_0}(u_{xx} - u_{yy}), \quad A_y(\mathbf{r}) = -\frac{2\beta t}{a_0}u_{xy}, \end{aligned} \quad (1)$$

where g is the deformation potential, t is the hopping energy, the parameter β is defined by $\beta = -\partial \log t / \partial \log a_0$, and a_0 is the lattice constant. In the following we consider one-dimensional periodicity of the deformation, and in view of Eq.(1) we assume that the periodic in x strain field generates periodic scalar and vector potentials $V(x)$ and $\mathbf{A}(x)$.

The Hamiltonian of electrons in graphene near the \mathcal{K} Dirac point in periodic scalar and vector fields reads

$$\mathcal{H} = -iv\boldsymbol{\sigma} \cdot (\nabla - i\mathbf{A}) + V, \quad (2)$$

where the Pauli matrices $\boldsymbol{\sigma}$ act on the sublattice label and we use the units $\hbar = e = 1$. This Hamiltonian describes low-energy excitations of the electronic system in graphene.

The corresponding Schrödinger equation for spinor wave function $\psi^T(\mathbf{r}) = (\varphi, \chi)$ is

$$\begin{pmatrix} \varepsilon - V & iv\partial_- + vA_- \\ iv\partial_+ + vA_+ & \varepsilon - V \end{pmatrix} \begin{pmatrix} \varphi \\ \chi \end{pmatrix} = 0, \quad (3)$$

where $\partial_{\pm} = \partial_x \pm i\partial_y$ and $A_{\pm} = A_x \pm iA_y$. Since the potentials $\mathbf{A}(x)$ and $V(x)$ do not depend on y and depend periodically on x , we take $\varphi, \chi \sim e^{i\mathbf{k}\cdot\mathbf{r}}$.

In frame of the $k \cdot p$ approximation²⁹, we have to calculate first the wavefunction $\psi(x)$ at $\mathbf{k} = 0$. The corresponding equations for the spinor components at $\mathbf{k} = 0$ are

$$(\varepsilon - V)\varphi + iv\chi' + vA_-\chi = 0, \quad (4)$$

$$iv\varphi' + vA_+\varphi + (\varepsilon - V)\chi = 0. \quad (5)$$

From Eq. (5) follows

$$\chi = -\frac{iv\varphi'}{\varepsilon - V} - \frac{vA_+\varphi}{\varepsilon - V}, \quad (6)$$

where prime means ∂_x . Substituting Eq.(6) into Eq.(4) we obtain the following equation for $\varphi(x)$

$$\begin{aligned} (\varepsilon - V)\varphi + \frac{v^2\varphi''}{\varepsilon - V} + \frac{v^2V'\varphi'}{(\varepsilon - V)^2} - \frac{iv^2A_+\varphi}{\varepsilon - V} - \frac{iv^2A_+\varphi'}{\varepsilon - V} \\ - \frac{iv^2V'A_+\varphi}{(\varepsilon - V)^2} - \frac{iv^2A_-\varphi'}{\varepsilon - V} - \frac{v^2A_+A_-\varphi}{\varepsilon - V} = 0. \end{aligned} \quad (7)$$

Let us assume the existence of solutions of Eq. (7) with $\varepsilon = 0$ (here we assume that $V \neq 0$). Then we get

$$\begin{aligned} \varphi'' - \left(\frac{V'}{V} + 2iA_x\right)\varphi' + \left(\frac{V^2}{v^2} - iA_+ + \frac{iV'A_+}{V} \right. \\ \left. - A_+A_-\right)\varphi = 0. \end{aligned} \quad (8)$$

This is the equation for $\varphi(x)$ in the \mathcal{K} Dirac point, corresponding to the lowest energy band.

Let us consider first some particular cases, when the periodic field is purely scalar $V(x)$ or purely vector field $\mathbf{A}(x)$.

A. Periodic scalar potential

In the case when $\mathbf{A}(x) = 0$ and $V(x) \neq 0$, Eq.(8) essentially simplifies to

$$\varphi'' - \frac{V'}{V}\varphi' + \frac{V^2}{v^2}\varphi = 0 \quad (9)$$

and has two different solutions

$$\varphi_{1,2}(x) = \exp\left(\pm \frac{i}{v} \int_0^x V(x') dx'\right). \quad (10)$$

Correspondingly, using Eqs.(6) and (10) we obtain

$$\chi_{1,2}(x) = \mp \exp\left(\pm \frac{i}{v} \int_0^x V(x') dx'\right). \quad (11)$$

Then the normalized basis functions in $k \cdot p$ approximation are

$$\psi_1(\mathbf{r}) = \frac{e^{i\mathbf{k}\cdot\mathbf{r}}}{\sqrt{2S}} \begin{pmatrix} \varphi_1 \\ \chi_1 \end{pmatrix}, \quad \psi_2(\mathbf{r}) = \frac{e^{i\mathbf{k}\cdot\mathbf{r}}}{\sqrt{2S}} \begin{pmatrix} \varphi_2 \\ \chi_2 \end{pmatrix}, \quad (12)$$

where $S = \mathcal{L}_x\mathcal{L}_y$ is the area of graphene sample. Calculating the matrix elements of the Hamiltonian (2) with basis functions (12) we find the effective Hamiltonian

$$\tilde{\mathcal{H}} = \begin{pmatrix} -vk_x & v(\gamma_1 k_x - \gamma_2 k_y) \\ v(\gamma_1 k_x - \gamma_2 k_y) & vk_x \end{pmatrix}, \quad (13)$$

where we denote

$$\gamma_1 = \frac{1}{L} \int_0^L dx \cos\left(\frac{2}{v} \int_0^x V(x') dx'\right), \quad (14)$$

$$\gamma_2 = \frac{1}{L} \int_0^L dx \sin\left(\frac{2}{v} \int_0^x V(x') dx'\right), \quad (15)$$

and L is the period of the potential $V(x)$. In correspondence with Eqs.(14) and (15) both parameters $\gamma_1, \gamma_2 < 1$.

The Hamiltonian (13) describes low-energy spectrum in the periodic scalar field. It has the following eigenvalues

$$\varepsilon_{1,2}(\mathbf{k}) = \pm v \sqrt{k_x^2 + (\gamma_1 k_x - \gamma_2 k_y)^2}. \quad (16)$$

Taking on alternate $k_y = 0$ and $k_x = 0$ we find that due to the periodic scalar field, the components of electron velocity in directions x and y , are renormalized, respectively, as $\tilde{v}_x/v = \sqrt{1 + \gamma_1^2}$ and $\tilde{v}_y/v = |\gamma_2|$. Thus, in this case we always obtain $v_x > v$ and $v_y < v$.

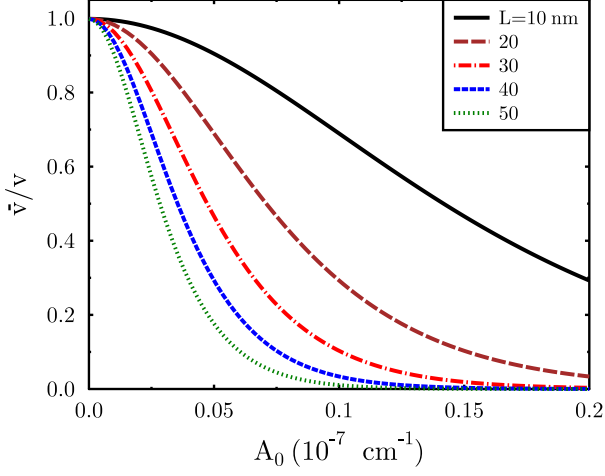


FIG. 1: Dependence of the renormalized velocity factor \tilde{v}/v on the amplitude A_0 of periodic potential $A_y(x)$ at different values of periodicity parameter L .

B. Periodic vector potential

In the case when $V(x) = 0$ and $\mathbf{A}(x) \neq 0$ we can use Eqs.(4) and (5) to find directly from these equations the spinor components of the wave function in the \mathcal{K} point, $\mathbf{k} = 0$

$$\begin{aligned}\varphi(x) &= \exp\left(i \int_0^x A_+(x') dx'\right), \\ \chi(x) &= \exp\left(i \int_0^x A_-(x') dx'\right).\end{aligned}\quad (17)$$

Then we can introduce two $k \cdot p$ basis functions in the form

$$\psi_1(\mathbf{r}) = N_1 e^{i\mathbf{k}\cdot\mathbf{r}} \begin{pmatrix} \varphi \\ 0 \end{pmatrix}, \quad \psi_2(\mathbf{r}) = N_2 e^{i\mathbf{k}\cdot\mathbf{r}} \begin{pmatrix} 0 \\ \chi \end{pmatrix}, \quad (18)$$

where N_i are the normalization factors

$$N_{1,2} = \left[\mathcal{L}_y \int_0^{\mathcal{L}_x} \exp\left(\mp 2 \int_0^x A_y(x') dx'\right) dx \right]^{-1/2}. \quad (19)$$

for the crystal of size $\mathcal{L}_x \times \mathcal{L}_y$. Calculating the matrix elements of the Hamiltonian (2) with $V(x) = 0$ in the basis of $k \cdot p$ functions (18) we get

$$\tilde{\mathcal{H}} = \begin{pmatrix} 0 & \tilde{v}k_- \\ \tilde{v}^*k_+ & 0 \end{pmatrix}, \quad (20)$$

where

$$\tilde{v} = v N_1 N_2 \mathcal{L}_y \int_0^{\mathcal{L}_x} \varphi^*(x) \chi(x) dx. \quad (21)$$

Using Eqs.(17) and (21) we finally obtain

$$\begin{aligned}\frac{\tilde{v}}{v} &= \left[\frac{1}{L^2} \int_0^L \exp\left(-2 \int_0^{x_1} A_y(x') dx'\right) dx_1 \right. \\ &\quad \left. \times \int_0^L \exp\left(2 \int_0^{x_2} A_y(x') dx'\right) dx_2 \right]^{-1/2}.\end{aligned}\quad (22)$$

The dependence of \tilde{v}/v from the amplitude A_0 of the periodic potential $A_y(x) = A_0 \sin(2\pi x/L)$ at different values of period L is presented in Fig. 1. The renormalized electron velocity decreases in the periodic vector field. This is in agreement¹⁸ with Ref. [16].

C. General case: both scalar and vector potentials are nonzero

In the general case when both $V(x) \neq 0$ and $\mathbf{A}(x) \neq 0$ we cannot find simple analytic solutions but we can analyze further Eq.(8) for $\varphi(x)$. For this purpose we present this equation as

$$\varphi'' + a\varphi' + b\varphi = 0, \quad (23)$$

where we denoted

$$a(x) = -\frac{V'}{V} - 2iA_x, \quad (24)$$

$$b(x) = \frac{V^2}{v^2} - iA'_+ + \frac{iV'A_+}{V} - A_+A_-. \quad (25)$$

Then after substitution

$$\varphi(x) = f(x) \exp\left(-\frac{1}{2} \int_0^x a(x') dx'\right) \quad (26)$$

we obtain the equation for the function $f(x)$

$$-\frac{1}{2} f'' + \left(\frac{a'}{4} + \frac{a^2}{8} - \frac{b}{2}\right) f = 0. \quad (27)$$

This is the Schrödinger equation for a particle of unit mass with energy $\varepsilon = 0$ in the potential

$$U(x) = -\frac{V''}{4V} + \frac{3(V')^2}{8V^2} + \frac{A_y^2 - A'_y}{2} + \frac{V'A_y}{2V} - \frac{V^2}{2v^2}. \quad (28)$$

Here we note that $U(x)$ does not depend on A_x . It can be used when $A_y = 0$ since in this case we can take the solution for $f(x)$ corresponding to $\varphi(x)$ from Eq. (10). This way we obtain simple generalization of Eqs. (10) and (11) for $A_x \neq 0$ and $A_y = 0$

$$\varphi_{1,2}(x) = \exp\left[i \int_0^x \left(\pm \frac{V(x')}{v} + A_x(x')\right) dx'\right], \quad (29)$$

$$\chi_{1,2}(x) = \mp \exp\left[i \int_0^x \left(\pm \frac{V(x')}{v} + A_x(x')\right) dx'\right]. \quad (30)$$

Turning back to Schrödinger equation (27) we also note that the potential (28) is real and periodic, $U(x) = U(x+L)$, so that we can present it as

$$U(x) = \sum_{n=1}^N \left(u_n e^{2\pi i n x/L} + u_n^* e^{-2\pi i n x/L} \right), \quad (31)$$

where the coefficients u_n can be found from the specific shape of potential $U(x)$.

We are looking for a periodic solution $f(x)$ of Eq.(27), which can be presented as

$$f(x) = \sum_m f_m e^{2\pi i m x/L} \quad (32)$$

with m is integer. Then using Eqs.(31), (32) and (27) we find the matrix equation for the coefficients f_m in Eq.(32)

$$\sum_m A_{nm} f_m = 0, \quad (33)$$

where $A_{nm} = \frac{1}{2} k_n^2 \delta_{nm} + u_{n-m} + u_{m-n}^*$ with $k_n = 2\pi n/L$ and $u_n = 0$ for any $n < 1$.

One can also look for the solution of Eq.(8) in the form $\varphi(x) = e^{is(x)}$. This representation can be more convenient for numerical calculations with arbitrary periodic functions $V(x)$ and $\mathbf{A}(x)$. In this approach we get the first order differential equation for $\xi(x)$

$$\xi' + i\xi^2 - \left(\frac{V'}{V} + 2iA_x \right) \xi - \frac{iV^2}{v^2} - A'_+ + \frac{V'A_+}{V} + iA_+A_- = 0, \quad (34)$$

where $\xi(x) = s'(x)$. Note that the transition to the case $V(x) \rightarrow 0$ formally corresponds to $V'/V \rightarrow \infty$ in Eq.(34).

One can assume that like Eqs.(12) and (18), in the general case there are also two solutions of Eq.(8) for the envelope function $\psi(x)$. Then there are also two different solutions of Eq.(34), $\xi_1(x)$ and $\xi_2(x)$. Correspondingly we get two solutions for the first spinor component

$$\varphi_i(x) = \exp \left(i \int_0^x \xi_i(x') dx' \right), \quad i = 1, 2.$$

Then using Eq.(6) with $\varepsilon = 0$ we find the other components $\chi_1(x)$ and $\chi_2(x)$. The obtained spinor function $(\varphi_i, \chi_i)^T$ should be properly normalized. As before, we use these independent solutions for our $k \cdot p$ basis presented by $\psi_i(\mathbf{r}) = N_i e^{i\mathbf{k}\cdot\mathbf{r}} (\varphi_i, \chi_i)^T$.

Thus, in the general case of arbitrary periodic perturbations we obtain the effective Hamiltonian

$$\tilde{\mathcal{H}} = \begin{pmatrix} 2v\alpha_1 k_x + 2v\alpha_2 k_y & v\gamma k_- + v\delta k_+ \\ v\gamma^* k_+ + v\delta^* k_- & 2v\beta_1 k_x + 2v\beta_2 k_y \end{pmatrix}, \quad (35)$$

where we denote

$$\begin{aligned} \alpha_1 + i\alpha_2 &= N_1^2 \mathcal{L}_y \int_0^{\mathcal{L}_x} \varphi_1^* \chi_1 dx, \\ \beta_1 + i\beta_2 &= N_2^2 \mathcal{L}_y \int_0^{\mathcal{L}_x} \varphi_2^* \chi_2 dx, \\ \zeta &= N_1 N_2 \mathcal{L}_y \int_0^{\mathcal{L}_x} \varphi_1^* \chi_2 dx, \\ \delta &= N_1 N_2 \mathcal{L}_y \int_0^{\mathcal{L}_x} \chi_1^* \varphi_2 dx. \end{aligned} \quad (36)$$

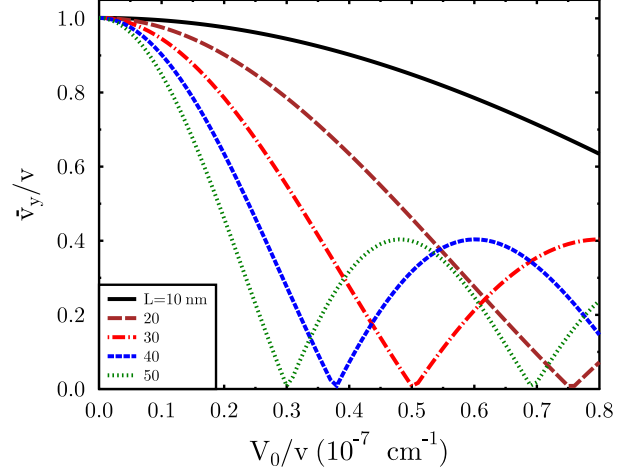


FIG. 2: Dependence of the renormalized velocity factor \tilde{v}_y/v on the amplitude of periodic scalar potential $V(x)$ at different values of periodicity parameter L .

The eigenvalues of Hamiltonian (35) are

$$\begin{aligned} \varepsilon_{1,2}(\mathbf{k}) &= v(\alpha_1 + \beta_1)k_x + v(\alpha_2 + \beta_2)k_y \\ &\pm v \left[(\alpha_1 - \beta_1)^2 k_x^2 + (\alpha_2 - \beta_2)^2 k_y^2 + (|\zeta|^2 + |\delta|^2) k^2 \right. \\ &\quad \left. + 2 \operatorname{Re}(\zeta\delta^*) (k_x^2 - k_y^2) + 4 \operatorname{Im}(\zeta\delta^*) k_x k_y \right]^{1/2}. \end{aligned} \quad (37)$$

For $k_x = 0$ we obtain $\varepsilon_{1,2}(k_y) = \tilde{v}_{1,2}^y k_y$, where

$$\tilde{v}_{1,2}^y/v = (\alpha_2 + \beta_2) \pm \left[(\alpha_2 - \beta_2)^2 + (|\zeta|^2 + |\delta|^2) - 2 \operatorname{Re}(\zeta\delta^*) \right]^{1/2}, \quad (38)$$

and for $k_y = 0$ we get $\varepsilon_{1,2}(k_x) = \tilde{v}_{1,2}^x k_x$, where

$$\tilde{v}_{1,2}^x/v = (\alpha_1 + \beta_1) \pm \left[(\alpha_1 - \beta_1)^2 + (|\zeta|^2 + |\delta|^2) + 2 \operatorname{Re}(\zeta\delta^*) \right]^{1/2}. \quad (39)$$

Using Eqs.(36), (38), and (39) one finds the components of electron velocity in graphene in the case of arbitrary periodic perturbation described by the fields $V(x)$ and $\mathbf{A}(x)$.

D. Longitudinal standing wave

For a longitudinal strain wave, the components of deformation are $u_x = u_x(x)$ and $u_y = 0$. Then in accordance with Eq.(1) we get $A_y = 0$ and due to Eq.(28) we can use the solutions (29) and (30).

Using Eq.(36) we find

$$\begin{aligned} \alpha &= -1/2, \quad \beta = 1/2, \\ \zeta &= -\delta = \frac{1}{2L} \int_0^L \exp \left(-\frac{i}{v} \int_0^x V(x') dx' \right) dx, \end{aligned} \quad (40)$$

and it follows from Eqs.(38) and (39) that $\tilde{v}_x = v$ and $\tilde{v}_y/v = 2|\zeta|$. The dependence of v_y/v on the amplitude of the periodic potential $V(x) = V_0 \sin(2\pi x/L)$ is shown in Fig. 2 for different values of periodicity parameter L .

E. Transversal standing wave

In case of transversal wave the only nonzero component of deformation is $u_y(x)$. Then in accordance with Eq.(1) we get $V(x) = 0$ and $A_x(x) = 0$. Correspondingly, the solutions for the components at $\mathbf{k} = 0$ are

$$\varphi_1(x) = \exp\left(-\int_0^x A_y(x') dx'\right), \quad \chi_1 = 0, \quad (41)$$

$$\varphi_2 = 0, \quad \chi_2(x) = \exp\left(\int_0^x A_y(x') dx'\right). \quad (42)$$

The solution for this case was already presented in Sec. 2B, see Eq.(22).

It should be noted that in reality the longitudinal and transverse phonon modes in graphene are not completely independent – there is some mixing between them²⁸. The above consideration is fully justified for the phonon (standing waves) with small q .

III. SCREENING

The scalar potential $V(x)$ generated by deformation wave in graphene is screened by electrons and holes. Screening is the main many-particle correction to the bare potential which should be taken into account.

For this purpose, using the RPA approximation, we calculate the loop diagram presenting the polarization operator³⁰

$$\Pi_0(\mathbf{q}) = -i \text{Tr} \int \frac{d^2\mathbf{k} d\varepsilon}{(2\pi)^3} G(\mathbf{k} + \mathbf{q}, \varepsilon) G(\mathbf{k}, \varepsilon), \quad (43)$$

where the Green function

$$G(\mathbf{k}, \varepsilon) = \frac{\varepsilon + \mu + v\boldsymbol{\sigma} \cdot \mathbf{k}}{(\varepsilon + \mu + i\delta \text{sgn} \varepsilon)^2 - \varepsilon_k^2} \quad (44)$$

corresponds to the Hamiltonian of graphene without any perturbations, μ is the chemical potential, and $\varepsilon_k = vk$. For definiteness we assume $\mu > 0$. This quantity has been calculated in many papers (see, e.g., Refs. [20,32–34]) but we present here some intermediate expressions to discuss a generalization to the anisotropic case.

Substituting Eq.(44) into Eq.(43) and integrating over ε we find

$$\Pi_0(\mathbf{q}) = \int \frac{d^2\mathbf{k}}{(2\pi)^2} \left\{ [f(\varepsilon_{\mathbf{k}+\mathbf{q}}) - f(\varepsilon_{\mathbf{k}})] \frac{\varepsilon_{\mathbf{k}+\mathbf{q}}^2 + \varepsilon_{\mathbf{k}}^2 + v^2\mathbf{k} \cdot \mathbf{q}}{\varepsilon_{\mathbf{k}+\mathbf{q}}(\varepsilon_{\mathbf{k}+\mathbf{q}}^2 - \varepsilon_{\mathbf{k}}^2)} + [1 - f(\varepsilon_{\mathbf{k}})] \frac{-\varepsilon_{\mathbf{k}+\mathbf{q}}\varepsilon_{\mathbf{k}} + \varepsilon_{\mathbf{k}}^2 + v^2\mathbf{k} \cdot \mathbf{q}}{\varepsilon_{\mathbf{k}}\varepsilon_{\mathbf{k}+\mathbf{q}}(\varepsilon_{\mathbf{k}+\mathbf{q}} + \varepsilon_{\mathbf{k}})} \right\}, \quad (45)$$

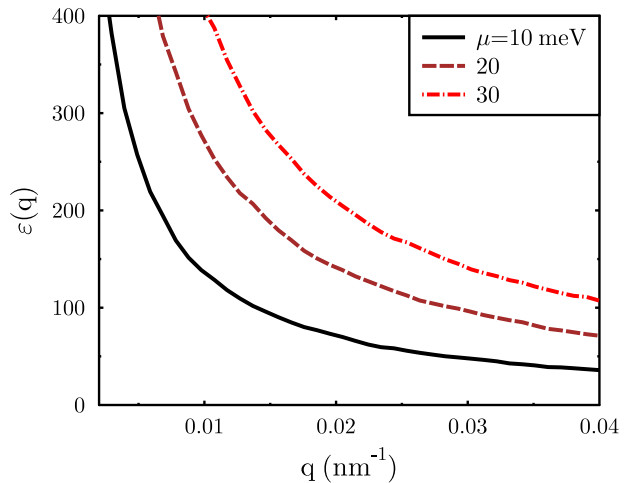


FIG. 3: Dependence of dielectric constant ε on q for different values of chemical potential μ .

where $f(\varepsilon) = \{ \exp[(\varepsilon - \mu)/T] + 1 \}^{-1}$ is the Fermi distribution function. In the limit of small $q \ll \mu/v$ we get

$$\Pi_0(\mathbf{q}) \simeq \int \frac{d^2\mathbf{k}}{(2\pi)^2} \frac{f(\varepsilon_{\mathbf{k}+\mathbf{q}}) - f(\varepsilon_{\mathbf{k}})}{\varepsilon_{\mathbf{k}+\mathbf{q}} - \varepsilon_{\mathbf{k}}}, \quad (46)$$

which gives us $\Pi_0(q \rightarrow 0) = -\nu(\mu)$, where $\nu(\varepsilon) = \varepsilon/2\pi v^2$ is the density of electron states with energy ε counted from the Dirac point. The second integral in Eq.(45) includes vacuum screening because it is nonzero at $\mu = 0$, i.e., in graphene without any carriers. In the limit of $q \rightarrow 0$ this contribution to $\Pi_0(\mathbf{q})$ disappears.

In frame of the RPA, the screened potential $V(q)$ is related to the bare potential $V_0(q)$ by $V(q) = V_0 + V_0 \Pi_0 u = V_0/\varepsilon$, where $u_0(q)$ and $u(q)$ refer respectively to bare and renormalized Coulomb interaction, and $\varepsilon(q) = 1 - u_0(q) \Pi_0(q)$. The dielectric constant $\varepsilon(q)$ calculated numerically using Eq.(45) is presented in Fig. 3. As we see in this figure, the scalar potential $V(q)$ is substantially suppressed by the screening since $\varepsilon(q) \gg 1$.

The same dielectric function $\varepsilon(q)$ determines (within the RPA) screening of the electron-electron interaction, $u(q) = u_0/\varepsilon$. The value of the effective screening radius is $R_c = -(2\pi e^2 \Pi_0(0))^{-1} = (2\pi e^2 \nu(\mu))^{-1}$.

In the periodic field, the components of velocity are renormalized, so that the density of states changes from $\nu(\varepsilon) = \varepsilon/(2\pi v^2)$ to $\tilde{\nu}(\varepsilon) = \varepsilon/(2\pi \tilde{v}_x \tilde{v}_y)$. Taking into account a variation of the chemical potential in the periodic field at a constant density of free carriers, $\tilde{\mu} = \mu \sqrt{\tilde{v}_x \tilde{v}_y}/v$ we find for the density of states at the Fermi level $\tilde{\nu} = \mu/(2\pi v \sqrt{\tilde{v}_x \tilde{v}_y})$. It means that $\tilde{\nu}$ grows with decreasing carrier velocity as $\tilde{\nu} \sim v/\sqrt{\tilde{v}_x \tilde{v}_y}$ leading to decreasing screening radius $R_c \sim \sqrt{\tilde{v}_x \tilde{v}_y}/v$. In other words, the periodic potential effectively enhances screening of the Coulomb interaction between electrons in graphene.

The periodic-field-induced variation of e-e interaction can affect the many-particle renormalization of the Fermi velocity³⁵⁻³⁷ due to modification of the screening. As follows from presented above estimations, this effect is especially important when $v/\sqrt{\tilde{v}_x\tilde{v}_y} \gg 1$.

On the other hand, the anisotropy of velocity generated by the periodic field can essentially modify the renormalization group (RG) equations of Refs. [35,37]. Indeed, by calculating the Fock self-energy diagram in the case of anisotropic spectrum with $\tilde{v}_x \neq \tilde{v}_y$ we find

$$\Sigma(\mathbf{k}) = \frac{e^2}{4\pi} \int_{|\mathbf{k}-\mathbf{q}|>k_F} \frac{d^2\mathbf{q}}{q} \frac{\tilde{v}_x\sigma_x(k_x - q_x) + \tilde{v}_y\sigma_y(k_y - q_y)}{\tilde{\varepsilon}_{\mathbf{k}-\mathbf{q}}},$$

where k_F is the Fermi wave vector, $\tilde{\varepsilon}_k = (\tilde{v}_x^2 k_x^2 + \tilde{v}_y^2 k_y^2)^{1/2}$. Correspondingly, the velocity correction is $\delta\tilde{v}_i = \delta\tilde{v}_i^{(1)} + \delta\tilde{v}_i^{(2)}$, where

$$\delta\tilde{v}_i^{(1)} = \frac{e^2\tilde{v}_i}{4\pi} \int_{|\mathbf{k}-\mathbf{q}|>k_F} \frac{d^2\mathbf{q}}{q} \frac{1}{\tilde{\varepsilon}_{\mathbf{k}-\mathbf{q}}}, \quad (47)$$

$$\delta\tilde{v}_i^{(2)} = -\frac{e^2\tilde{v}_i}{4\pi k^2} \int_{|\mathbf{k}-\mathbf{q}|>k_F} \frac{d^2\mathbf{q}}{q} \frac{\mathbf{k} \cdot \mathbf{q}}{\tilde{\varepsilon}_{\mathbf{k}-\mathbf{q}}}. \quad (48)$$

In Eq. (47) we take the limit $k \rightarrow 0$

$$\delta\tilde{v}_i^{(1)} = \frac{e^2\tilde{v}_i}{4\pi} \int_{k_F} \frac{dq}{q} \int_0^{2\pi} \frac{d\theta}{\sqrt{\tilde{v}_x^2 \cos^2 \theta + \tilde{v}_y^2 \sin^2 \theta}}, \quad (49)$$

whereas in (48) we have to take first $\mathbf{k} = (k, 0)$ for $\delta\tilde{v}_x^{(2)}$ and $\mathbf{k} = (0, k)$ for $\delta\tilde{v}_y^{(2)}$, respectively, and after that take the limit of $k \rightarrow 0$

$$\begin{aligned} \delta\tilde{v}_x^{(2)} &= -\frac{e^2\tilde{v}_x}{4\pi} \int_{k_F} \frac{dq}{q} \int_0^{2\pi} \frac{\tilde{v}_x^2 \cos^2 \theta d\theta}{(\tilde{v}_x^2 \cos^2 \theta + \tilde{v}_y^2 \sin^2 \theta)^{3/2}}, \\ \delta\tilde{v}_y^{(2)} &= -\frac{e^2\tilde{v}_y}{4\pi} \int_{k_F} \frac{dq}{q} \int_0^{2\pi} \frac{\tilde{v}_y^2 \sin^2 \theta d\theta}{(\tilde{v}_x^2 \cos^2 \theta + \tilde{v}_y^2 \sin^2 \theta)^{3/2}} \end{aligned} \quad (50)$$

The integrals over q in (49),(50) run from k_F to $q_{max} \simeq 1/a_0$. Since the field-induced renormalization of velocity refers only to region of small $q < 1/L$, we will divide each of these integrals to the part from k_F to $1/L$ (where, as we found, the spectrum is anisotropic), and to the part from $1/L$ to $1/a_0$ with $\tilde{v}_x = \tilde{v}_y = v$.

Let us assume for definiteness that for the bare values $\tilde{v}_x/\tilde{v}_y \leq 1$. Using (49),(50) and dividing each of integrals over q in two parts we find the following many-particle corrections to the velocity

$$\begin{aligned} \delta\tilde{v}_x &\simeq \frac{e^2\xi_0}{4} + \frac{e^2\tilde{v}_x\xi}{\pi\tilde{v}_y} \left[\mathbf{K}(m) - \frac{\tilde{v}_x^2}{\tilde{v}_y^2} \mathbf{R}(m) \right], \\ \delta\tilde{v}_y &\simeq \frac{e^2\xi_0}{4} + \frac{e^2\xi}{\pi} [\mathbf{K}(m) - \mathbf{P}(m)], \end{aligned} \quad (51)$$

where we denoted $\xi_0 = \log(L/a_0)$, $\xi = \log(1/k_FL)$, $\mathbf{K}(m) = \int_0^{\pi/2} (1 - m \sin^2 \theta)^{-1/2} d\theta$

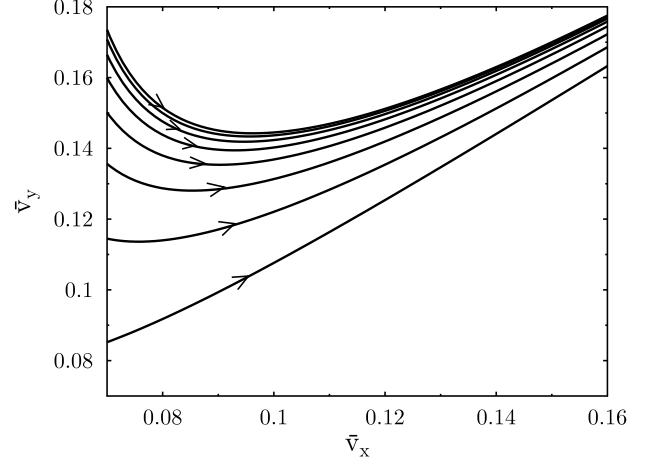


FIG. 4: The characteristics of RG Eqs. (52). In the limit of $\tilde{v}_x \rightarrow 0$, all of them go to ∞ . The renormalization due to the e-e interaction shifts the initial values of $\tilde{v}_x + e^2\xi_0/4$ and $\tilde{v}_y + e^2\xi_0/4$ along a certain characteristic to the right.

(complete elliptic integral of the 1st kind³⁸), $\mathbf{P}(m) = \int_0^{\pi/2} (1 - m \sin^2 \theta)^{-3/2} \sin^2 \theta d\theta$, $\mathbf{R}(m) = \int_0^{\pi/2} (1 - m \sin^2 \theta)^{-3/2} \cos^2 \theta d\theta$, and $m = 1 - \tilde{v}_x^2/\tilde{v}_y^2$. As we are interested in the limit of small k_F , the integrals over q are calculated with the logarithmic precision assuming $k_F \ll 1/L \ll 1/a_0$.

The first terms in the right hand sides of (51) lead to a constant shift of the bare values $\tilde{v}_i \rightarrow \tilde{v}_i + e^2\xi_0/4$. Note that in the limit of $\tilde{v}_x = \tilde{v}_y$, Eqs. (51) coincide with the ones from Refs. [35,37].

Using (51) we obtain the following RG equations

$$\begin{aligned} \frac{\partial\tilde{v}_x}{\partial\xi} &= \frac{e^2\tilde{v}_x\xi}{\pi\tilde{v}_y} \left[\mathbf{K}(m) - \frac{\tilde{v}_x^2}{\tilde{v}_y^2} \mathbf{R}(m) \right], \\ \frac{\partial\tilde{v}_y}{\partial\xi} &= \frac{e^2\xi}{\pi} [\mathbf{K}(m) - \mathbf{P}(m)]. \end{aligned} \quad (52)$$

The corresponding characteristics in the sector $0 < \tilde{v}_x < \tilde{v}_y$ of $(\tilde{v}_x, \tilde{v}_y)$ plane are presented in Fig. 4. As we see, the e-e-interaction-induced renormalization leads to the effective isotropization of the energy spectrum, which has been broken by the periodic field.

IV. PLASMONS

First we calculate the real part of polarization operator $\Pi_0(\mathbf{q}, \omega)$ for $\omega \neq 0$ assuming that $\varepsilon_k = vk$. It allows to consider the plasmons in graphene (corresponding to the poles of dielectric function $\varepsilon(\omega, \mathbf{q})$) without external perturbations,

$$\text{Re } \Pi_0(\mathbf{q}, \omega) = - \int \frac{d^2\mathbf{k}}{(2\pi)^2} \left\{ [1 - f(\varepsilon_{\mathbf{k}+\mathbf{q}})] \right.$$

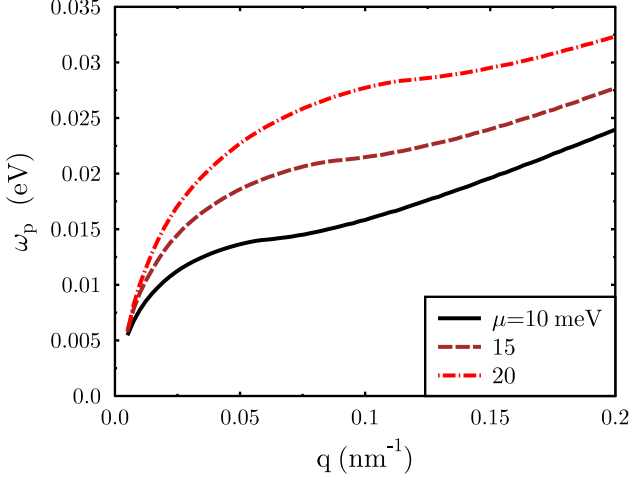


FIG. 5: Plasmon spectrum $\omega_p(q)$ of graphene for different values of the chemical potential μ .

$$\times \frac{\varepsilon_{\mathbf{k}+\mathbf{q}}(\varepsilon_{\mathbf{k}+\mathbf{q}} - \omega) + \varepsilon_{\mathbf{k}}^2 + v^2 \mathbf{k} \cdot \mathbf{q}}{\varepsilon_{\mathbf{k}+\mathbf{q}}[(\varepsilon_{\mathbf{k}+\mathbf{q}} - \omega)^2 - \varepsilon_{\mathbf{k}}^2]} + [1 - f(\varepsilon_{\mathbf{k}})] \frac{2\varepsilon_{\mathbf{k}}^2 + \varepsilon_{\mathbf{k}}\omega + v^2 \mathbf{k} \cdot \mathbf{q}}{\varepsilon_{\mathbf{k}}[(\varepsilon_{\mathbf{k}} + \omega)^2 - \varepsilon_{\mathbf{k}+\mathbf{q}}^2]} \}. \quad (53)$$

The dielectric function $\varepsilon(\mathbf{q}, \omega) = 1 - \frac{2\pi e^2}{q} \text{Re} \Pi_0(\mathbf{q}, \omega)$ can be found using polarization operator (53). The plasmon spectrum is calculated by solving numerically equation $\varepsilon(\mathbf{q}, \omega_p) = 0$. It is presented in Fig. 5. At small $q \ll \mu/v$ the spectrum is $\omega_p(q) \sim \sqrt{q}$ in agreement with Refs. [21,39]. As we see from Fig. 5, at larger q the plasmon dispersion is linear with q . When $\mu \rightarrow 0$, the plasmon spectrum is linear.

As we demonstrated in Sec. II, the energy spectrum of low-energy excitations in graphene under the periodic perturbation can be described by an effective Hamiltonian (35). After some unitary transformation T this Hamiltonian can be reduced to the form similar of non-perturbed graphene

$$T^{-1} \tilde{\mathcal{H}} T = \tilde{v}_x \sigma_x k_x + \tilde{v}_y \sigma_y k_y. \quad (54)$$

with renormalized values of electron velocity. For example, in the case of longitudinal standing wave, we have $T = e^{-i\pi\sigma_y/4}$, $\tilde{v}_x = v$ and $\tilde{v}_y = 2v|\zeta|$ with ζ defined by Eq. (40).

The polarization operator $\text{Re} \Pi(\mathbf{q}, \omega)$ in the periodic field can be found using the same formula (53) after scaling transformation $k_i = (v/\tilde{v}_i) \tilde{k}_i$ and $q_i = (v/\tilde{v}_i) \tilde{q}_i$. Then we find

$$\text{Re} \Pi(\tilde{\mathbf{q}}, \omega) = \frac{v^2}{\tilde{v}_x \tilde{v}_y} \text{Re} \Pi_0(\tilde{\mathbf{q}}, \omega). \quad (55)$$

Since the renormalization of electron velocities is different for longitudinal and transversal waves, the plasmon spectrum is different in these cases, too.

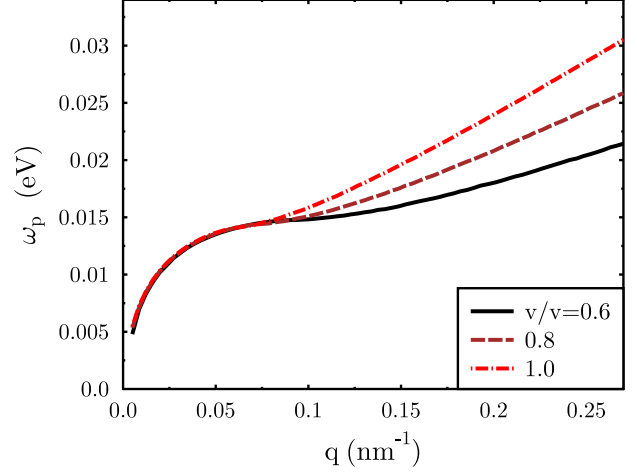


FIG. 6: Plasmon spectrum $\omega_p(q)$ of graphene under periodic perturbation for different values of the electron velocity (without anisotropy like in the case of periodic vector potential). Here the chemical potential $\mu = 10$ meV.

As shown before, the plasmon spectrum at $q \rightarrow 0$ is proportional to \sqrt{q} . It corresponds to $\text{Re} \Pi_0(q, \omega) \sim q^2/\omega^2$. Then the scaling transformation presented above does not change the polarization operator at $q \rightarrow 0$. Thus, the variation of electron velocity does not affect the plasmon spectrum at small q .

In Fig. 6 we present the results of numerical calculation of the plasmon spectrum for different values of renormalized velocity \tilde{v}/v . It corresponds, e.g., to the presence of periodic field $A_y(x)$. This figure demonstrates that only the linear part of the spectrum can be strongly affected by the periodic field.

In the case of longitudinal wave and in the limit of $q \rightarrow 0$ we obtain

$$\text{Re} \Pi(\tilde{q}, \omega) \simeq C(\omega) \left(\frac{v q_x^2}{\tilde{v}_y} + \frac{\tilde{v} q_y^2}{v} \right). \quad (56)$$

It leads to the anisotropy of plasmonic spectrum.

V. ROLE OF INTERVALLEY TRANSITIONS

It should be pointed out that our consideration of the plasmonic spectrum cannot be extended to q of the order of the vector of inverse lattice. The point is that when one starts from the tight-binding approximation to describe the electronic structure of graphene, the Hamiltonian of the Coulomb interaction has the following form (index σ labels sublattices A and B)

$$\begin{aligned} H_{int} &= \sum_{\mathbf{R}_\sigma \mathbf{R}'_{\sigma'}} c_{\mathbf{R}_\sigma}^\dagger c_{\mathbf{R}_\sigma} u_0(\mathbf{R}_\sigma - \mathbf{R}'_{\sigma'}) c_{\mathbf{R}'_{\sigma'}}^\dagger c_{\mathbf{R}'_{\sigma'}} \\ &= \sum_{\mathbf{k} \mathbf{k}' \mathbf{q} \sigma \sigma'} c_{\mathbf{k}\sigma}^\dagger c_{\mathbf{k}-\mathbf{q},\sigma} u_0(\mathbf{q}) c_{\mathbf{k}'\sigma'}^\dagger c_{\mathbf{k}'+\mathbf{q},\sigma'}, \end{aligned} \quad (57)$$

where \mathbf{k} and \mathbf{k}' are any points in the Brillouin zone. Considering the states near the Dirac points \mathcal{K} and \mathcal{K}' we can present (57) in a different form

$$H_{int} = \sum_{\mathbf{k}\mathbf{k}'\mathbf{q}\sigma\sigma'ij} [c_{\mathbf{k}\sigma i}^\dagger c_{\mathbf{k}-\mathbf{q},\sigma i} u_0(\mathbf{q}) c_{\mathbf{k}'\sigma'j}^\dagger c_{\mathbf{k}'+\mathbf{q},\sigma'j} + c_{\mathbf{k}\sigma i}^\dagger c_{\mathbf{k}-\mathbf{q},\sigma j} u_0(\mathbf{q}-\mathbf{Q}) c_{\mathbf{k}'\sigma'j}^\dagger c_{\mathbf{k}'+\mathbf{q},\sigma'i}], \quad (58)$$

where i, j labels the valleys, \mathbf{k} and \mathbf{k}' are measured from the corresponding Dirac points, and \mathbf{Q} is the vector between the points \mathcal{K} and \mathcal{K}' . This expression shows that for plasmon excitations with momentum of the order of Q , intervalley transitions should be taken into account, as was pointed out in Ref. [22].

VI. CONCLUSION

We considered the variation of electron energy spectrum near the Dirac point in graphene under periodic perturbation related to the scalar and vector gauge fields, which can be generated by the periodic deformations. The possible source of such deformation fields is a periodic strain wave like in the case of the ultrasonic wave in solid. We found that in the general case with both $V \neq 0$ and $\mathbf{A} \neq 0$ there exist solution for the renormal-

ized electron velocity, corresponding to the anisotropy of the spectrum. The problem substantially simplifies in some particular cases. Namely, for pure longitudinal and pure transverse periodic excitations the solutions have simple form.

We also considered the screening of the scalar potential and found that it is strongly suppressed, especially at small q . It means that the main perturbation affecting the electron velocity is the vector potential \mathbf{A} .

We calculated the plasmon spectrum of collective excitations in graphene in the presence of periodic excitations. We found that the plasmon spectrum can be strongly affected by the periodic field. For the longitudinal excitations, one appears the anisotropy of plasmon spectrum.

Acknowledgements

This work is supported by the Deutsche Forschungsgemeinschaft in Germany, by the National Science Center as a research project in years 2011 – 2014 in Poland, and by the "Stichting voor Fundamenteel Onderzoek der Materie (FOM)", which is financially supported by the "Nederlandse Organisatie voor Wetenschappelijk Onderzoek (NWO)".

-
- ¹ A. K. Geim and K. S. Novoselov, *Nature Mater.* **6**, 183 (2007).
- ² A. H. Castro Neto, F. Guinea, N. M. R. Peres, K. S. Novoselov, and A. K. Geim, *Rev. Mod. Phys.* **81**, 109 (2009).
- ³ M. I. Katsnelson, *Graphene: Carbon in Two Dimensions* (Cambridge Univ. Press, Cambridge, 2012).
- ⁴ P. Avouris, Z. Chen, and V. Perebeinos, *Nature Nanotech.* **2**, 605 (2007).
- ⁵ A. K. Geim, *Science* **324**, 1530 (2009).
- ⁶ F. Bonaccorso, Z. Sun, T. Hasan, and A. C. Ferrari, *Nat. Photon.* **4**, 611 (2010).
- ⁷ K. S. Novoselov, *Rev. Mod. Phys.* **83**, 837 (2011).
- ⁸ M. Jablan, H. Buljan, and M. Soljačić, *Phys. Rev. B* **80**, 245435 (2009).
- ⁹ A. A. Dubinov, V. Ya. Aleshkin, V. Mitin, T. Otsuji, and V. Ryzhii, *J. Phys. Cond. Matter.* **23**, 145302 (2011).
- ¹⁰ V. M. Pereira and A. H. Castro Neto, *Phys. Rev. Lett.* **103**, 046801 (2009).
- ¹¹ F. Guinea, M. I. Katsnelson, and A. K. Geim, *Nat. Phys.* **6**, 30 (2010).
- ¹² F. Guinea, A. K. Geim, M. I. Katsnelson, and K. S. Novoselov, *Phys. Rev. B* **81**, 035408 (2010).
- ¹³ M. A. H. Vozmediano, M. I. Katsnelson, and F. Guinea, *Phys. Rep.* **496**, 109 (2010).
- ¹⁴ C. H. Park, L. Yang, Y. W. Son, M. L. Cohen, and S. G. Louie, *Phys. Rev. Lett.* **101**, 126804 (2008).
- ¹⁵ C. H. Park, L. Yang, Y. W. Son, M. L. Cohen, and S. G. Louie, *Nature Phys.* **4**, 213 (2008).
- ¹⁶ L. Z. Tan, C. H. Park, and S. G. Louie, *Phys. Rev. B* **81**, 195426 (2010).
- ¹⁷ M. Yankowitz, J. Xue, D. Cormode, J. D. Sanchez-Yamagishi, K. Watanabe, T. Taniguchi, P. Jarillo-Herrero, P. Jacquod, and B. J. LeRoy, *Nature Phys.* **8**, 382 (2012).
- ¹⁸ Discussing the effect of vector potential Tan et al.¹⁶ used Lorentz transformation to imaginary electric field with the subsequent analytic continuation to the real field. In our method we use the standard quantum mechanics. Even though our numerical results are in agreement, analytical formulas are slightly different. In particular, our Eq. (22) shows that the change of electron velocity does not depend on the sign of periodic perturbation.
- ¹⁹ S. Wu, M. Killi, and A. Paramekanti, *Phys. Rev. B* **85**, 195404 (2012).
- ²⁰ E. H. Hwang and S. Das Sarma, *Phys. Rev. B* **75**, 205418 (2007).
- ²¹ S. Das Sarma and E.H. Hwang, *Phys. Rev. Lett.* **102**, 206412 (2009).
- ²² T. Tudorovskiy and S. A. Mikhailov, *Phys. Rev. B* **82**, 073411 (2010).
- ²³ A. Yu. Nikitin, F. Guinea, T. J. García-Vidal, and L. Martín-Moreno, *Phys. Rev. B* **84**, 161407(R) (2011).
- ²⁴ S. H. Abedinpour, G. Vignale, A. Principe, M. Polini, W. K. Tse, and A. H. MacDonald, *Phys. Rev. B* **84**, 045429 (2011).
- ²⁵ S. Yuan, R. Roldan, and M. I. Katsnelson, *Phys. Rev. B* **84**, 035439 (2011).
- ²⁶ P. K. Pyatkovskiy and V. P. Gusynin, *Phys. Rev. B* **83**, 075422 (2011).
- ²⁷ H. Suzuura and T. Ando, *Phys. Rev. B* **65**, 235412 (2002).

- ²⁸ J. L. Mañes, Phys. Rev. B **76**, 045430 (2007).
- ²⁹ I. M. Tsidilkovskii, *Band Structure of Semiconductors* (Pergamon, Oxford, 1982).
- ³⁰ We use matrix Green's functions, which automatically accounts for correct matrix elements of e-e interaction and includes possible vacuum screening of the filled valence bands. This method has been used for similar calculations in narrow-gap semiconductors³¹.
- ³¹ A. A. Abrikosov, Zh. Eksp. Teor. Fiz. **66**, 1443 (1974) [Sov. Phys. JETP **39** (1974)].
- ³² E. V. Gorbar, V. P. Gusynin, V. A. Miransky, and I. A. Shovkovy, Phys. Rev. B **66**, 045108 (2002).
- ³³ T. Ando, J. Phys. Soc. Japan **75**, 074716 (2006).
- ³⁴ B. Wunsch, T. Stauber, F. Sols, and F. Guinea, New J. Phys. **8**, 318 (2006).
- ³⁵ J. Gonzalez, F. Guinea, and M. A. H. Vozmediano, Phys. Rev. B **59**, 2474(R) (1999).
- ³⁶ M. S. Foster and I. L. Aleiner, Phys. Rev. B **77**, 195413 (2008).
- ³⁷ D. C. Elias, R. V. Gorbachev, A. S. Mayorov, S. V. Morozov, A. A. Zhukov, P. Blake, L. A. Ponomarenko, I. V. Grigorieva, K. S. Novoselov, F. Guinea, and A. K. Geim, Nature Phys. **7**, 701 (2011).
- ³⁸ M. Abramowitz and I. A. Stegun, *Handbook of Mathematical Functions*, Natl. Bur. Stand. Appl. Math. Ser. 55 (Natl. Bur. Stand., Washington, DC, 1964).
- ³⁹ E. H. Hwang, R. Sensarma, and S. Das Sarma, Phys. Rev. B **82**, 195406 (2010).